JTTEE5 16:776–782
DOI: 10.1007/s11666-007-9126-4
1059-9630/$19.00 © ASM International

Peer Reviewed

Microstructural Analysis and Photocatalytic Activity of Plasma-Sprayed Titania-Hydroxyapatite Coatings

F.-X. Ye, A. Ohmori, T. Tsumura, K. Nakata, and C.-J. Li

(Submitted March 12, 2007; in revised form August 31, 2007)

Hydroxyapatite (HAp $Ca_{10}(PO_4)_6(OH)_2$) is known to be a biomaterial and an adsorbent for chromatography. In this study, HAp was agglomerated with anatase TiO_2 to manufacture thermal-spray powders to improve the adsorption activity of TiO_2, and then to improve its photocatalytic activity. The microstructures, compositions and photocatalytic activity of plasma-sprayed TiO_2, TiO_2-10%HAp, TiO_2-30%HAp, and HAp coatings were investigated. Due to the low thermal conductivity of HAp compound, not all HAp particles fully melted even under the arc current of 800 A. The addition of HAp inhibited the phase transformation of anatase TiO_2 to rutile. Under the arc current of 600 A, the anatase content in the TiO_2, TiO_2-10%HAp and TiO_2-30%HAp coatings was 11, 20 and 42%, respectively. With the increasing of the spraying distance from 70 to 110 mm, the anatase content in the TiO_2-30%HAp coatings decreased from 34 to 17% under arc current of 700 A. Furthermore, a slight decomposition of HAp to α-$Ca_3(PO_4)_2$ was found in the TiO_2-30%HAp coatings, it did not decompose to CaO and P_2O_5 according to the XRD and EDAX analysis. The addition of the secondary gas of helium had no significant influence on the melting state of the TiO_2-HAp feedstock powders. Moreover, the HAp in the TiO_2-10%HAp and TiO_2-30%HAp coatings had adsorption characteristic to acetaldehyde. The photocatalytic activity of TiO_2-10%HAp coating was highest among TiO_2, TiO_2-10%HAp, and TiO_2-30%HAp coatings sprayed under the arc current of 600 A for the optimum adsorption property and anatase content.

Keywords hydroxyapatite, photocatalyst, plasma spray, TiO_2

1. Introduction

In order to purify the polluted environment and avoid further pollution, photocatalysis has been attracting great attention since the discovery of Fujishima and Honda phenomenon in 1972 (Ref 1). When the photocatalyst is illuminated with photons, whose energy is equal to or greater than its band-gap energy, hydroxyl radical will generate in common. The hydroxyl radical energy is 501 kJ/mol, which is higher than the general bonding energy, such as C-C, N-H, C-O, etc. Therefore, most organic substances and bacteria can be oxidized by photocatalyst to simple species, such as CO_2, H_2O, etc. Over the past 30 years of research from 1972, TiO_2 has proved to be the promising one due to its strong oxidizing power under UV illumination and its chemical stability. TiO_2 crystallizes in three major different structures: rutile (tetragonal), anatase (tetragonal), and brookite (rhombohedrical). As a photocatalyst, anatase TiO_2 shows higher photocatalytic activity (Ref 2-11). However, TiO_2 tends to photochemically decompose other materials, such as organic paint, textile, and plastics, when they exist together with it. Furthermore, it can only decompose substances that have come into contact, and this decomposition will not work in the dark.

In contrast, hydroxyapatite (HAp $Ca_{10}(PO_4)_6(OH)_2$) is generally chemically inert, and very known to be a practical biomaterial and an adsorbent for chromatography or pollutant collection. It also exhibits thermal catalytic activities in many chemical reactions (Ref 12-17).

Therefore, a multifunctional ceramic composite material of TiO_2 and HAp was developed by plasma-spraying technique in this study. The following characteristics are expected. (1) the HAp adsorbs contaminants even without irradiation to light; (2) material adsorbed by the HAp is decomposed by the TiO_2 photocatalyst on exposure to light; (3) the HAp is used as an inert spacer, allowing

This article is an invited paper selected from presentations at the 2007 International Thermal Spray Conference and has been expanded from the original presentation. It is simultaneously published in *Global Coating Solutions, Proceedings of the 2007 International Thermal Spray Conference*, Beijing, China, May 14-16, 2007, Basil R. Marple, Margaret M. Hyland, Yuk-Chiu Lau, Chang-Jiu Li, Rogerio S. Lima, and Ghislain Montavon, Ed., ASM International, Materials Park, OH, 2007.

F.-X. Ye, School of Materials Science & Engineering, Tianjin University, Weijin Road No. 92, Tianjin, 300072, P.R. China; **A. Ohmori**, TOCALO Co. Ltd., Minamifutami, Futami-Cho, Akashi, Japan; **T. Tsumura** and **K. Nakata**, Joining and Welding Research Institute, Osaka University, Osaka, Japan; and **C.-J. Li**, Welding Research Institute, School of Materials Science & Engineering, Xi'an Jiaotong University, Shaanxi, P.R. China. Contact e-mail: yefx@tju.edu.cn; yefx77@gmail.com

blending the material with resins, organic coatings, and other organic materials; (4) though the photocatalyst requires some time to fully decompose organic materials, adsorption of contaminants by the HAp ensures complete decomposition (Ref 12).

In order to elucidate the influence of HAp on the microstructures, compositions and photocatalytic activity of plasma-sprayed TiO_2-HAp coatings, anatase TiO_2, TiO_2-10%HAp, TiO_2-30%HAp, and HAp powders were designed. The microstructures, compositions, and photocatalytic activity of the sprayed HAp and TiO_2-HAp coatings were discussed in details.

2. Materials and Experimental Procedures

2.1 Feedstock Powders and Substrate

HAp particles with average primary size of 5 μm were agglomerated to HAp feedstock powder with average size of 33 μm. Anatase TiO_2 particles with an average primary size of 200 nm were agglomerated to anatase TiO_2 feedstock powder with an average size of 33 μm. In order to manufacture TiO_2-10%HAp and TiO_2-30%HAp feedstock powders, TiO_2 particle with average size of 200 nm was mechanically and uniformly mixed with 5 μm HAp particles with corresponding weight ratio. The average size of TiO_2-10%HAp, and TiO_2-30%HAp feedstock powders was approximated to 33 μm. The X-ray diffraction patterns of the TiO_2, TiO_2-10%HAp, TiO_2-30%HAp and HAp feedstock powders are shown in Fig. 1. The morphology of TiO_2-30%HAp powder is given in Fig. 2, which was very similar to the other powders used in this study. The substrate was stainless steel (JIS SUS304).

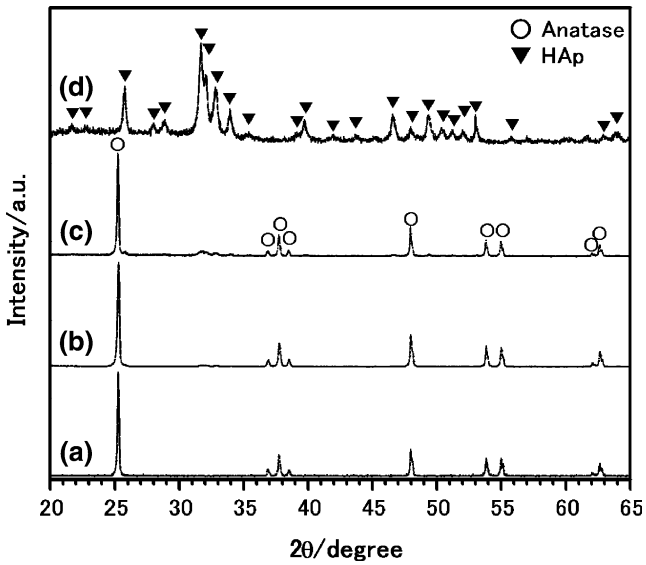

Fig. 1 X-ray diffraction patterns of the TiO_2 (a), TiO_2-10%HAp (b), TiO_2-30%HAp (c) and HAp (d) feedstock powders

2.2 Plasma Spraying Equipment

The thermal-spraying equipment was a plasma-spraying system (Plasmadyne-Mach1, Miller Thermal, USA). Argon was applied as primary gas, and helium was applied as secondary gas. The thermal spraying parameters are given in Table 1. If the spraying distance and helium gas pressure are not specially given in the spraying parameters in this article, they were 70 mm and 0.21 MPa, respectively.

2.3 Characterization of Powders and Sprayed Coatings

Electron-probe surface roughness analyzer (ERA-8800FE, Elionix Co. Ltd., Japan) and energy dispersive analysis of x-ray (EDAX) were used to examine the structure characteristics of the feedstock powders and the sprayed coatings. The phase composition of the feedstock powders and the sprayed coatings was investigated by X-ray diffraction using Cu-Kα radiation (λ = 1.5406 Å) and graphite crystal monochromator (M03XHF, MAC Science Co. Ltd.). The content of anatase phase in the sprayed coatings was calculated using the most common equation given by Spurr and Myers (Ref 18).

$$A = \frac{1}{1 + 1.265\,(I_R/I_A)} \times 100\% \qquad \text{(Eq 1)}$$

where I_A is the highest peak intensity of anatase phase (101 peak), I_R the highest peak intensity of rutile phase (110 peak) and A the content of anatase phase in the sprayed coatings.

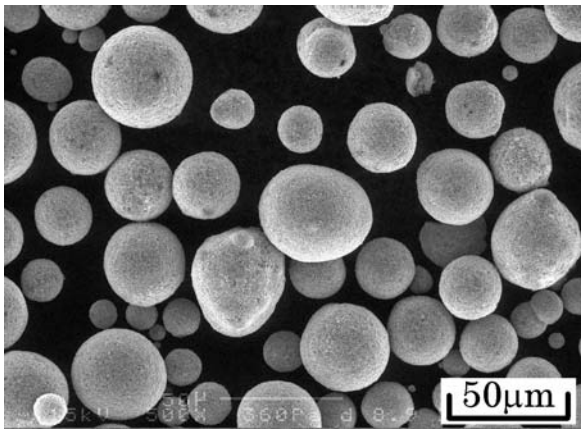

Fig. 2 Typical morphology of TiO_2-30%HAp feedstock powder

Table 1 Plasma-spray parameters for a Plasma Dyne spray system

Argon gas pressure, MPa	0.42
Argon gas flow, slpm	58
Helium gas pressure, MPa	0, 0.21, 0.42
Helium gas flow, slpm	0, 9, 18
Arc current, A	600, 700, 800
Arc voltage, V	28-30
Spraying distance, mm	70, 90, 110

It is known that surface roughness will affect the photocatalytic performance, the surface roughness of TiO_2, TiO_2-10%HAp, TiO_2-30%HAp, and HAp coatings was investigated by a surface roughness analyzer (DEKTAK, ULVAC, Japan).

The concentration of acetaldehyde gas under dark or irradiation condition was measured by a Kitakawa gas detector at a certain time interval to evaluate the adsorption and decomposition characteristics of the sprayed TiO_2 and TiO_2-HAp coatings. The experimental set up and procedure were elsewhere given in details (Ref 10, 19).

2.4 Definition of Relative Deposition Rate of Feedstock Powder

In thermal-spray technology, there have many parameters to evaluate the properties of sprayed coatings, such as cohesion strength, hardness, wear resistance, powder deposition efficiency, and so on. The mechanical properties of sprayed coatings are very important in mechanical applications. However, great attention should be paid on not only the functional performance but also the powder deposition rate in the developments of functional coatings. Therefore, to evaluate the fabrication characteristics of the feedstock powder at various plasma-spraying conditions, the powder deposition rate was defined as Eq 2. The calculated result was applied to compare the powder deposition efficiency in this study.

$$\mathrm{RDRP} = \frac{T_{\mathrm{Thickness}} V_{\mathrm{Traverse}} W_{\mathrm{Step}}}{n V_{\mathrm{Rotation}}} \quad \text{(Eq 2)}$$

where RDRP is Relative Deposition Rate of Powder, V_{Rotation} relative rotation speed of powder feeder, V_{Traverse} relative traverse speed of plasma gun, W_{Step} relative step width of up-down moving equipment, $T_{\mathrm{Thickness}}$ thickness of sprayed coating, n spray pass of the coating.

3. Results and Discussion

3.1 Typical Microstructure of HAp and TiO_2-30%HAp Coatings

Figure 3 shows the surface morphologies and cross sections of HAp coatings sprayed under the arc current of 600, 700, and 800 A. It indicates that the unmelted particles decreased and the coating became denser with the increasing of arc current. Although the ceramic powder with high melting point might be totally melted under the plasma power of 24 kW (800 A, 30 V), there still existed unmelted particles for HAp powder. The melting state of the particles in the plasma jet is influenced by the particle size, the thermal conductivity, the flight time of the powder, and the temperature of plasma jet and so on. The thermal conductivity of HAp is 1.4 $Wm^{-1}K^{-1}$, while 10.4 and 180.0 $Wm^{-1}K^{-1}$ for rutile and anatase TiO_2, respectively (Ref 20-22). It is concluded the much low thermal conductivity of HAp was the main reason to affect HAp particles' melting state.

The arithmetical mean deviation of the surface profile (Ra) of the TiO_2, TiO_2-10%HAp, TiO_2-30%HAp, and HAp coatings sprayed under the arc current of 600 A was 6.3, 6.9, 7.3 and 7.8 μm, respectively. For the lower thermal conductivity and larger primary particle size of HAp than that of TiO_2, the surface roughness of the sprayed TiO_2 coating increased slightly with the addition of HAp.

Figure 4 shows the relative deposition rate of the HAp feedstock powders (RDRP). It increased with the increasing of arc current for the higher energy of plasma jet. Under the arc current of 600 A, the RDRP of HAp powder was 11 μm/pass, which was very low. As shown in Fig. 5, the RDRP of TiO_2 powder under the arc current of 600 A was approximated to 60 μm/pass. Although the thermal conductivity of HAp is lower than that of TiO_2, the addition of 10%HAp to TiO_2 improved powder deposition efficiency slightly for the large primary size of HAp. With more HAp addition, the thermal conductivity became more important factor to affect RDRP, and then the RDRP of TiO_2-30%HAp powder decreased.

The Ca/P ratio is an important quantity for calcium phosphate ceramics, and this may change during the plasma spraying process (Ref 17). The typical EDAX pattern of TiO_2-30%HAp coatings plasma sprayed under the highest power input in this study (arc current: 800 A, helium gas pressure: 0.42 MPa) is shown in Fig. 6. The weight intensity of Ca/P for the coating was 2.19, which was in good agreement with that of powder. This means that the HAp did not decomposed completely to CaO and P_2O_5 and P did not evaporate, or else the value would increase. However, intermediate products such as α-tricalcium phosphate appeared even under the relative low power input (arc current: 600 A, helium gas pressure: 0.21 MPa) as discussed in the next section.

3.2 Compositions of Plasma Sprayed Coatings

Tricalcium phosphate (TCP: Ca_3PO_4) has three polymorphs: Low temperature β-TCP, which is stable below 1350 K, while α-TCP is stable between 1350 and 1673 K, and α′-TCP is observed above 1740 K (Ref 17, 22). The *hkl* of the highest peak of β-TCP is 217 and the 2θ is 31.0321° for Cu-Kα radiation. They are 170 and 30.7558° while for α-TCP.

Figure 7 illustrates XRD patterns of plasma sprayed HAp coatings under the arc current of 600, 700, and 800 A. A new peak appeared at 31.0321°, which means β-TCP existed in the coatings. It is reported that the Ca-deficient HAp transforms to the low temperature polymorph of β-TCP with loss of water upon heating to 973–1073 K (Ref 23, 24). α-TCP was not detected even under the arc current of 800 A.

Figure 8 illustrates XRD patterns of plasma sprayed TiO_2-30%HAp coatings under the arc current of 600 A. A new peak appeared at 30.7558°, which means α-TCP existed in the coatings. Since α-TCP was detected even under the arc current of 600 A, it implied that the temperature of the particle was over 1350 K for good thermal conductivity of TiO_2, and the heat was transferred to HAp from TiO_2.

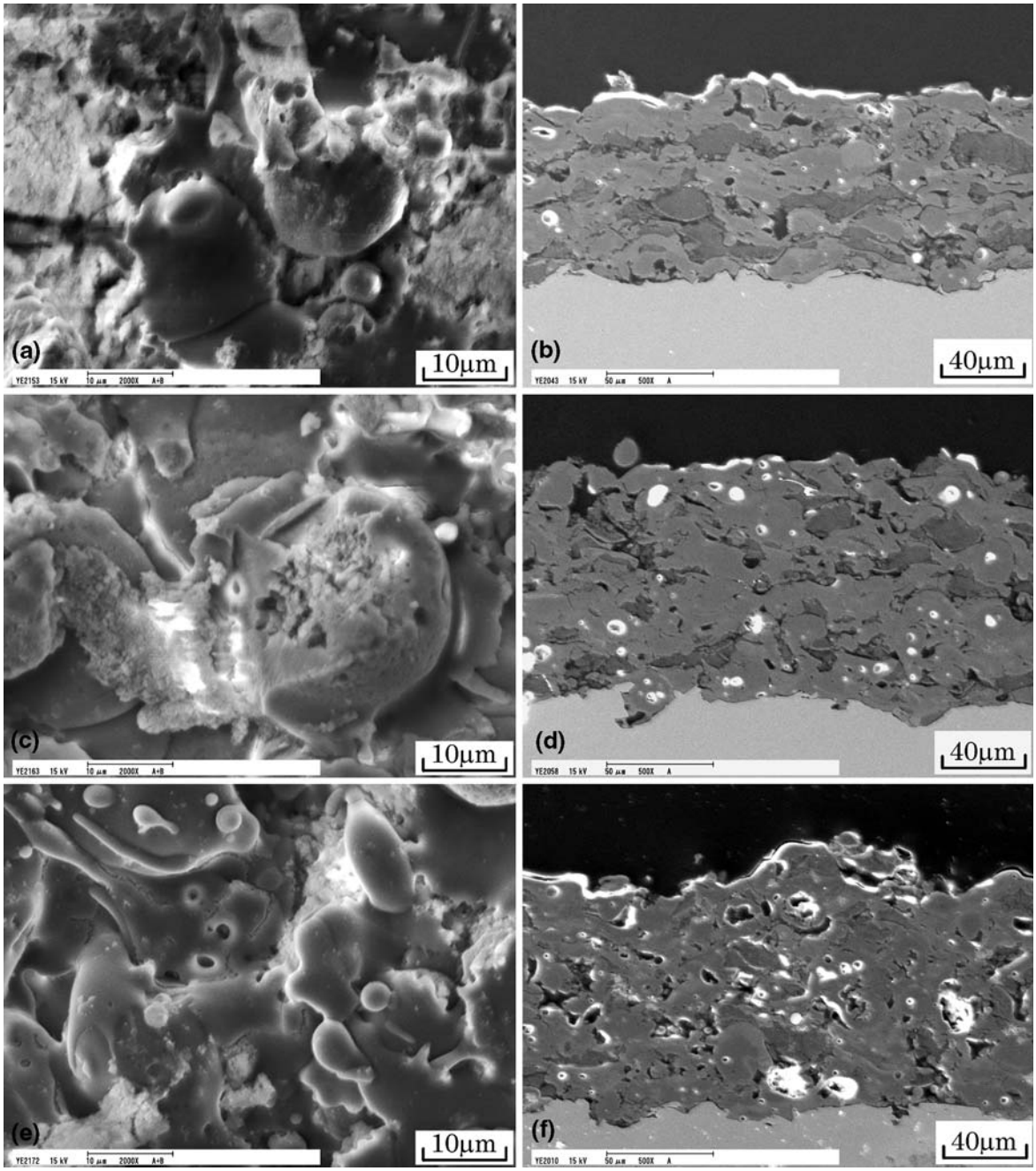

Fig. 3 Morphologies and cross sections of HAp coatings plasma sprayed under the arc current of 600 A (a, b), 700 A (c, d) and 800 A (e, f)

3.3 Content of Anatase Phase and Photocatalytic Activity of the Sprayed TiO_2-HAp Coatings

The anatase content in the TiO_2-30%HAp coating was calculated by Eq 1. Under the arc current of 600 A, the anatase content in the TiO_2, TiO_2-10%HAp and TiO_2-30%HAp coatings was 11, 20 and 42%, respectively. Under the arc current of 700 A, it decreased from 34 to 17% for the TiO_2-30%HAp coatings with the increasing of spraying distance from 70 to 110 mm for the longer in-flight time in plasma jet as shown in Fig. 9. The higher anatase content will tend to improve the photocatalytic activity of the coatings. In order to inhibit the anatase TiO_2 transformation to rutile and to keep high anatase content in the coatings, the spraying distance of 70 mm was better than that of 90 and 110 mm.

Generally, the addition of the secondary gas of helium to argon will increase the enthalpy of plasma and then improve the RDRP. The influence of anatase content in the sprayed TiO_2-30%HAp coatings with the helium

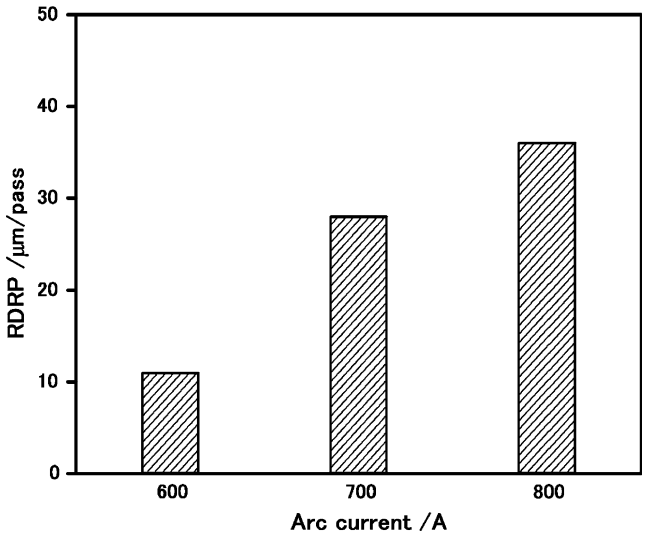

Fig. 4 Relative deposition rate of HAp powder (RDRP) under the spraying distance of 70 mm and helium gas pressure of 0.21 MPa

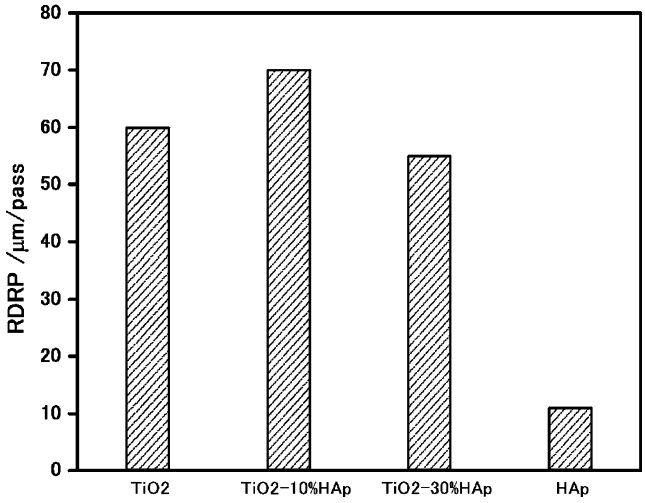

Fig. 5 Relative deposition rate of TiO_2, TiO_2-10%HAp, TiO_2-30%HAp and HAp feedstock powders under the arc current of 600 A, spraying distance of 70 mm and helium gas pressure of 0.21 MPa

pressure is shown in Fig. 10. Although significant change was not observed, it decreased gradually with the addition of helium gas.

Figure 11 illustrates the adsorption and decomposition characteristics of TiO_2, TiO_2-10%HAp, and TiO_2-30%HAp coatings. When the light was turn off (Experimental time from 0 to 1.5 h), the concentration of acetaldehyde with TiO_2 coating had a little change. While the concentration of acetaldehyde with TiO_2-10%HAp, TiO_2-30%HAp coatings decreased 8 and 13% in 0.5 h, respectively, and then shifted to a constant. This decrease mainly resulted from the adsorption characteristic of HAp in the TiO_2-10%HAp and TiO_2-30%HAp

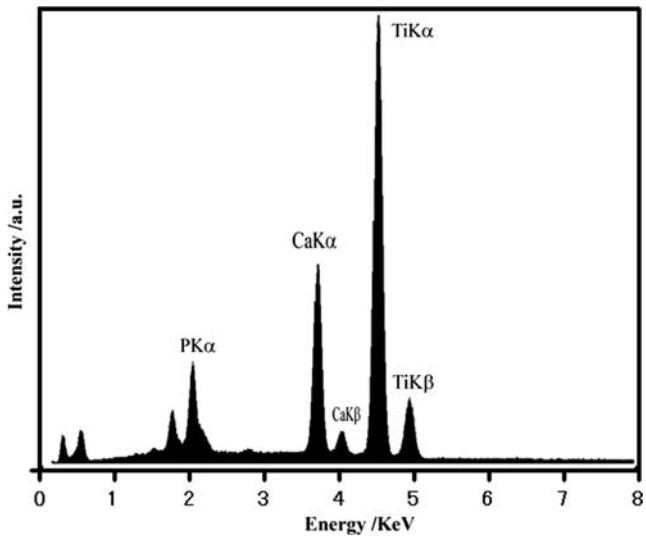

Fig. 6 EDAX pattern of TiO_2-30%HAp coating plasma sprayed under the arc current of 800 A, spraying distance of 70 mm and helium gas pressure of 0.42 MPa

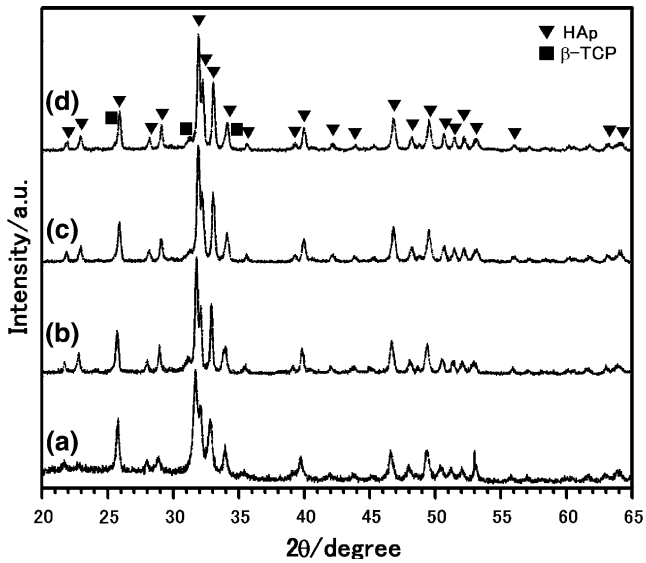

Fig. 7 XRD patterns of HAp powder (a), and HAp coatings plasma sprayed under the arc current of 600 A (b), 700 A (c) and 800 A (d) (Spraying distance: 70 mm, Helium gas pressure: 0.21 MPa)

coatings. When the light was turn on, concentration of acetaldehyde decreased with irradiation time and the photocatalytic activity of TiO_2-10%HAp coating was highest for the optimum adsorption property and anatase content.

4. Conclusions

The microstructures, compositions and photocatalytic activity of plasma sprayed TiO_2, TiO_2-10%HAp,

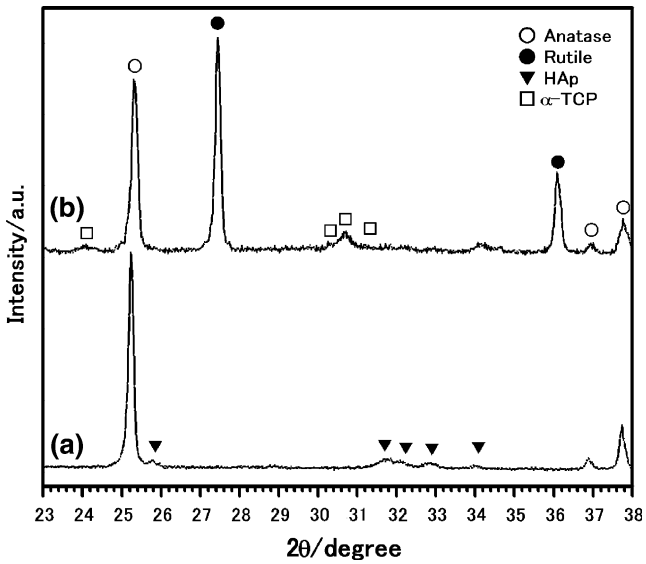

Fig. 8 X-ray diffraction patterns of the TiO_2-30%HAp powder (a) and coatings (b) plasma sprayed under the arc current of 600 A

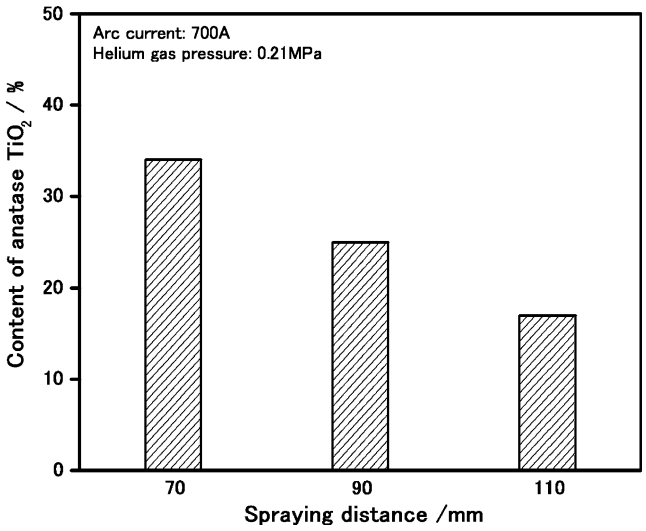

Fig. 9 The anatase content in the TiO_2-30%HAp coatings under the arc current of 700 A, helium gas pressure of 0.21 MPa and different spraying distance

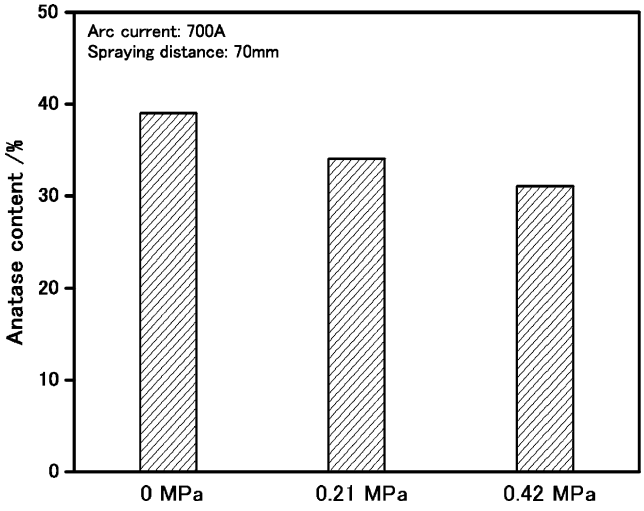

Fig. 10 The anatase content in the TiO_2-30%HAp coatings sprayed under the arc current of 700 A, spraying distance of 70 mm and different helium gas pressure

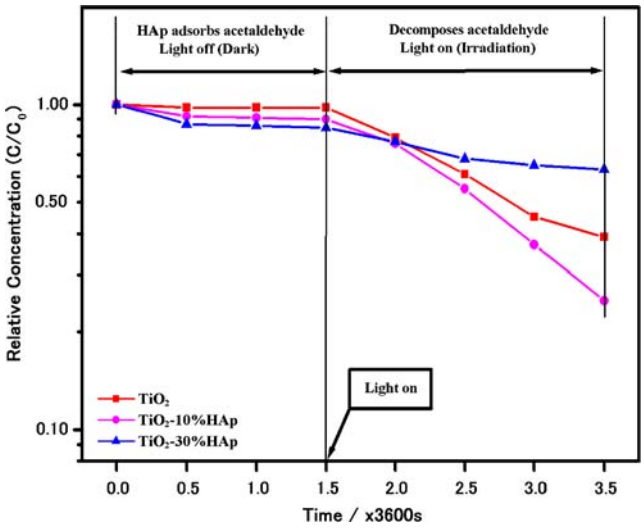

Fig. 11 The adsorption and decomposition characteristics of TiO_2, TiO_2-10%HAp, TiO_2-30%HAp coatings plasma sprayed under the arc current of 600 A

TiO_2-30%HAp and HAp coatings were investigated. Due to the low thermal conductivity of the HAp compound, not all HAp particles fully melted even under the arc current of plasma power input of 24 kW. The addition of HAp inhibited the phase transformation of anatase TiO_2 to rutile. With the increasing of the spraying distance from 70 to 110 mm, the anatase content in the TiO_2-30%HAp coatings decreased from 34 to 17% under arc current of 700 A. Furthermore, low temperature stable β-$Ca_3(PO_4)_2$ was detected in the sprayed HAp coatings. Although slightly decomposition of HAp to α-$Ca_3(PO_4)_2$ was observed in the TiO_2-30%HAp coatings sprayed under high-plasma power input, it did not decompose to CaO and P_2O_5 according to the XRD and EDAX analysis. The addition of the secondary gas of helium had no significant influence on the melting state of the TiO_2-HAp feedstock powders. Moreover, the HAp in the TiO_2-10%HAp and TiO_2-30%HAp coatings had adsorption characteristic to acetaldehyde. The photocatalytic activity of TiO_2-10%HAp coating was highest among TiO_2, TiO_2-10%HAp and TiO_2-30%HAp coatings sprayed under the arc current of 600 A for the optimum adsorption property and anatase content.

References

1. A. Fujishima and K. Honda, Electrochemical Photolysis of Water at a Semiconductor Electrode, *Nature*, 1972, **238**(5358), p 37-38
2. H. Tributsch and L. Pohlmann, Synergetic Molecular Approaches towards Artificial and Photosynthetic Water Photoelectrolysis, *J. Electroanal. Chem.*, 1995, **396**, p 53-61
3. A. Fujishima, T.N. Rao, and D.A. Tryk, Titanium Dioxide Photocatalysis, *J. Photochem. Photobio. C: Photobio. Rev.*, 2000, **1**(1), p 1-21
4. A. Mills and S.L. Hunte, An Overview of Semiconductor Photocatalysis, *J. Photochem. Photobio. A Chem.*, 1997, **108**, p 1-35
5. K. Pirkanniemi and M. Sillanpaa, Heterogeneous Water Phase Catalysis as an Environmental Application: A Review, *Chemosphere*, 2002, **48**, p 1047-1060
6. J. Zhao and X.D. Yang, Photocatalytic Oxidation for Indoor Air Purification: A Literature Review, *Build. Environ.*, 2003, **38**, p 645-654
7. J.M. Herrmann, Heterogeneous Photocatalysis: Fundamentals and Applications to the Removal of Various Types of Aqueous Pollutants, *Catal. Today*, 1999, **53**, p 115-129
8. S. Malato, J. Blanco, A. Vidal, and C. Richter, Photocatalysis with Solar Energy at a Pilot-plant Scale: An Overview, *Appl. Catal. B-Environ.*, 2002, **37**, p 1-15
9. P. Fernandez-Ibanez, S. Malato, and O. Enea, Photoelectrochemical Reactors for the Solar Decontamination of Water, *Catal. Today*, 1999, **54**, p 329-339
10. F.X. Ye and A. Ohmori, The Photocatalytic Activity and Photoabsorption of Plasma Sprayed TiO_2-Fe_3O_4 Binary Oxide Coatings, *Surf. Coat. Technol.*, 2002, **160**(1), p 62-67
11. F.X. Ye, A. Ohmori, and C.J. Li, New Approach to Enhance the Photocatalytic Activity of Plasma Sprayed TiO_2 Coatings Using *p-n* Junctions, *Surf. Coat. Technol.*, 2004, **184**, p 233-238
12. T. Nonami, H. Hase, and K. Funakoshi, Apatite-coated Titanium Dioxide Photocatalyst for Air Purification, *Catal. Today*, 2004, **96**, p 113-118
13. A. Nakajima, K. Takakuwa, and Y. Kameshima, et al., Preparation and Properties of Titania-Apatite Hybrid Films, *J. Photochem. Photobio. A Chem.*, 2006, **177**, p 94-99
14. Y. Wang, K.A. Khor, and P. Cheang, Thermal Spraying of Functionally Graded Calcium Phosphate Coatings for Biomedical Implants, *J. Therm. Spray. Technol.*, 1998, **7**(1), p 50-57
15. J.D. Haman, A.A. Boulware, L.C. Lucas, and D.E. Crawmer, High-velocity Oxyfuel Thermal Spray Coatings for Biomedical Applications, *J. Therm. Spray. Technol.*, 1995, **4**(2), p 179-184
16. P. Cheang and K.A. Khor, Influence of Powder Characteristics on Plasma Sprayed Hydroxyapatite Coatings, *J. Therm. Spray. Technol.*, 1996, **5**(3), p 310-316
17. K.A. Khor, C.S. Yip, and P. Cheang, Ti-6Al-4V/hydroxyapatite Composite Coatings Prepared by Thermal Spray Techniques, *J. Therm. Spray. Technol.*, 1997, **6**(1), p 109-115
18. R.A. Spurr and H. Myers, Quantitative Analysis of Anatase-Rutile Mixtures with an x-ray Diffactometer, *Anal. Chem.*, 1957, **29**(5), p 760-762
19. A. Ohmori, F.X. Ye, and C. J. Li, The Effects of the Additives on Photocatalytic Performance of Plasma Sprayed Titanium Dioxide Coatings, *International Thermal Spray Conference*, E. Lugscheider and C.C. Berndt, Ed., March 4-6, Essen, Germany, DVS, 2002, p 165-169
20. S. Dyshlovenko, B. Pateyron, L. Pawlowski, and D. Murano, Numerical Simulation of Hydroxyapatite Powder Behaviour in Plasma Jet, *Surf. Coat. Technol.*, 2004, **179**, p 110-117
21. http://www.matweb.com/search/SpecificMaterial.asp?bassnum=BOTiA
22. http://www.astlettrubber.com/pdf/titaniumdioxide/msds/titaniumdioxide.pdf
23. H.S. Ryu, H.J. Youn, K.S. Kong, B.S. Chang, C.K. Lee, and S.S. Chung, An Improvement in Sintering Property of β-Tricalcium Phosphate by Addition of Calcium Pyrophosphate, *Biomaterials*, 2003, **23**, p 909-914
24. D. Choi and P.N. Kumta, Mechano-chemical Synthesis and Characterization of Nanostructured β-TCP Powder, *Mat. Sci. Eng. C*, 2007, **27**(3), p 377-381